Journal of Inorganic and General Chemistry
ZAAC
Zeitschrift für anorganische und allgemeine Chemie
www.zaac.wiley-vch.de
RESEARCH ARTICLE

DOI: 10.1002/zaac.202200107

Keeping dysprosium in line: Trinuclear heterometallic $M^{II}_2Dy^{III}$ complexes with M = Cd, Co and Cu

Thomas Ruppert,[a] Sören Schlittenhardt,[b] Nithin Suryadevara,[b] Olaf Fuhr,[b, c] Christopher E. Anson,[a] Mario Ruben,[b, d] and Annie K. Powell*[a, b, d]

Dedicated to Prof. Dr. Dieter Fenske on the occasion of his 80th birthday.

Four new heterometallic trinuclear essentially linear ("in-line") $M^{II}_2Dy^{III}$ complexes (M = Cd^{II} (**1**), Co^{II} (**2**), Cu^{II} (**3**, **4**) were synthesised using the ligand 3,5-di-*tert*-butylbenzoic acid (dtbbaH) in a MeCN:^{i}PrOH (**1–3**) or in a MeOH:^{i}PrOH:DMF (**4**) mixture. Single crystal structure analyses revealed the formation of $[Cd_2Dy(dtbba)_6(^iPrOH)_2(H_2O)_2NO_3]\cdot{}^iPrOH$ (**1**), $[Co_2Dy(dtbba)_6(^iPrOH)_2(H_2O)_2NO_3]\cdot{}^iPrOH$ (**2**), $[Cu_2Dy(dtbba)_6(MeCN)_4NO_3]\cdot MeCN$ (**3**) and $[Cu_2Dy(dtbba)_6(^iPrOH)_{1.68}(DMF)_{1.32}(H_2O)NO_3]\cdot 3{}^iPrOH\cdot H_2O$ (**4**). The M–Dy–M angles become more acute from (**1**) to (**3**) leading to decreased M··M distances. The Dy^{III} ions are 8-coordinate with a distorted triangular dodecahedron geometry and a D_{2d} symmetry whereas the geometry of the 5-coordinate terminal M^{II} ions can best be described as either distorted vacant octahedra or as spherical square pyramids with a C_{4v} symmetry. Magnetic susceptibility measurements were performed on (**1**), (**2**) and (**3**) which allows a comparison of the effect of replacing highly anisotropic Co^{II} with the quantum spin of Cu^{II}. Both (**2**) and (**3**) show effects of ferromagnetic interactions at low temperatures.

Introduction

A major interest in the synthesis of 3d-4f coordination compounds lies in the possibility of slow relaxation of magnetisation and thus so-called single molecule magnet (SMM) behaviour.[1–6] The very first 3d-4f complex showing SMM behaviour – a $[Cu^{II}Tb^{III}]$ system – was reported in 2004.[7] This was the beginning of many publications in the area of 3d-4f compounds such as the bell-shaped $[Mn_{11}Gd_2]$[8] arrangement, the "square-in-square" $[Mn^{III}_4Ln^{III}_4]$[9] structures, three-dimensional $[Ln^{III}_4Co^{II}_3]$[10] systems, "in-line" $[Dy^{III}_2Co^{III}]$[11] compounds or butterfly shaped $M^{II}_2Ln^{III}_2$ schemes including M = Co^{II} or Cu^{II} ions.[12,13] The exchange of the 3d metal ions in these systems with a diamagnetic species such as Zn^{II} or Co^{III} in the same row of the Periodic Table allows the contribution of the lanthanide ion(s) to be assessed.[14–16] However, it was possible to exchange the paramagnetic 3d metals with the diamagnetic 4d ion Cd^{II} which is a good diamagnetic alternative for Zn^{II}. In addition to the magnetic properties of such systems many reasons exist as to why it is intriguing to investigate transition metal lanthanide 3d/4f and 4d/4f systems. For example, the combined properties of SMM and luminescent behaviour in a dinuclear ZnLn compound,[17] water oxidation and photocatalytic effects of LnTi systems[18,19] as well as optical properties in a 4d-4f-3d complex[20] have been reported.

There are several synthetic strategies to form these systems including one-pot synthesis with or without *in situ* formation of organic ligands,[21,22] solvo- and hydrothermal reactions,[21,23] as well as self-assembly methods.[24] Many linear, or more generally "in-line", trinuclear M_2Ln (M = 3d or 4d ions) systems exist in the literature. These are mostly synthesised using Schiff-base ligands[25–28] with oxygen- and nitrogen-rich coordination pockets respectively for the lanthanides and the 3d/4d ions resulting in a mixed atom coordination environment for the metal ions. There are rare examples of systems where the ions are only bridged through the oxygen atoms of a single ligand.[24,29] Here we present the syntheses and molecular structures of four new heterometallic $M^{II}_2Ln^{III}$ complexes with the formulae $[Cd_2Dy(dtbba)_6(^iPrOH)_2(H_2O)_2NO_3]\cdot{}^iPrOH$ (**1**) $[Cd_2Dy]$, $[Co_2Dy(dtbba)_6(^iPrOH)_2(H_2O)_2NO_3]\cdot{}^iPrOH$ (**2**) $[Co_2Dy]$, $[Cu_2Dy$-

[a] *Dr. T. Ruppert, Dr. C. E. Anson, Prof. Dr. A. K. Powell*
Institute for Inorganic Chemistry (AOC), Karlsruhe Institute of Technology (KIT),
Engesserstr. 15, 76131 Karlsruhe, Germany
E-mail: annie.powell@kit.edu
[b] *S. Schlittenhardt, Dr. N. Suryadevara, Dr. O. Fuhr, Prof. Dr. M. Ruben, Prof. Dr. A. K. Powell*
Institute of Nanotechnology (INT), Karlsruhe Institute of Technology (KIT),
Hermann-von-Helmholtz-Platz 1, 76344 Eggenstein-Leopoldshafen, Germany
[c] *Dr. O. Fuhr*
Karlsruhe Nano Micro Facility (KNMFi),
Hermann-von-Helmholtz-Platz 1, 76344 Eggenstein-Leopoldshafen, Germany
[d] *Prof. Dr. M. Ruben, Prof. Dr. A. K. Powell*
Institute for Quantum Materials and Technologies (IQMT), Karlsruhe Institute of Technology (KIT),
Hermann-von-Helmholtz-Platz 1, 76344 Eggenstein-Leopoldshafen, Germany

Supporting information for this article is available on the WWW under https://doi.org/10.1002/zaac.202200107

$(dtbba)_6(MeCN)_4NO_3]\cdot MeCN$ (**3**) $[Cu_2Dy–MeCN]$ and $[Cu_2Dy(dtbba)_6(^iPrOH)_{1.68}(DMF)_{1.32}(H_2O)NO_3]\cdot 3^iPrOH\cdot H_2O$ (**4**) $[Cu_2Dy–DMF]$ (with dtbbaH = 3,5-di-*tert*-butylbenzoic acid). Additionally, magnetic susceptibility measurements were performed on (**1**), (**2**) and (**3**) to investigate the nature of magnetic interactions within the systems. For the systems discussed here the heteronuclear Zn^{II}-Dy^{III} compound could not be isolated successfully and was therefore not further investigated. The synthesis using zinc nitrate did not result in the desired Zn_2Dy complex but rather in a dysprosium chain with the ligand 3,5-di-*tert*-butylbenzoic acid.

Results and Discussion

Structural description. The metal ions are in an "in-line" M–Ln–M arrangement with M–Dy–M angles all greater than 161°. The metals are linked by six *syn*,*syn*-bridging $dtbba^-$ ligands. A chelating nitrate completes the coordination environment of the dysprosium, while terminal solvent ligands complete the square-pyramidal coordination spheres of the M^{II} ions (Figure 1).

The $[Cd_2Dy]$ complex (**1**) and $[Co_2Dy]$ (**2**) are isostructural and crystallise in the monoclinic space group C2/c, whereas (**3**) and (**4**) crystallise in the triclinic space group P-1. The asymmetric unit of (**1**) and (**2**) contains half the molecule which corresponds to half a Dy^{III} with half a chelating nitrate and one M^{II} ion (M = Cd for (**1**) and Co for (**2**)) plus three bridging $dtbba^-$ ligands (dtbbaH = 3,5-di-*tert*-butylbenzoic acid), one coordinated ^iPrOH and one coordinated H_2O on the M^{II} ion. Therefore, the ratio of organic ligand:^iPrOH:H_2O:NO_3^- in the molecular structure (**1**) and (**2**) is 6:2:2:1.

On the other hand, the asymmetric units within the triclinic space group P-1 for $[Cu_2Dy–MeCN]$ (**3**) and $[Cu_2Dy–DMF]$ (**4**) contain the whole molecule. In (**3**), the coordinated ^iPrOH and H_2O molecules on the Cu^{II} ions are replaced by MeCN. The coordinated species on the Cu^{II} ions in (**4**) are either one ^iPrOH and one H_2O (on Cu1) or one ^iPrOH and one DMF (on Cu2). In these structures the "in-line" metal ions have M–Dy–M angles of 170.72(1)° in (**1**), 165.40(3)° in (**2**), 165.25(1)° in (**3**) and 161.48(1)° in (**4**). Due to the closest approach to linearity, the Cd··Cd distances in (**1**) are the longest at 7.5826(4) Å. The Co··Co distances in (**2**) (7.5526(21) Å) are longer than the Cu··Cu distances in (**3**) with 7.4808(6) Å and (**4**) with 7.5409(4) Å. The Dy^{III} ions are bridged to the M^{II} ions via the carboxylate oxygen atoms of the three $dtbba^-$ ligands. The M··Dy distances are 3.8037(2) Å in (**1**), 3.8075(10) Å in (**2**), 3.7516(4) and 3.7916(5) Å in (**3**) and 3.8332(3) and 3.8072(3) Å, respectively, in (**4**). With the bidentate coordinated NO_3^- this leads to 8-coordinate Dy^{III} ions with an O_8 environment and a D_{2d} symmetry around the Dy^{III} ion best described as a triangular dodecahedron (TDD). The Dy–O bond lengths range from 2.277(2) Å to 2.543(2) Å in (**1**), 2.246(5) to 2.545(5) Å in (**2**), 2.258(2) to 2.500(3) Å in (**3**) and 2.2716(16) to 2.4933(19) Å in (**4**). The M^{II} ions in (**1**)-(**4**) are coordinated by the oxygens of three bridging $dtbba^-$ ligands with Cd–O bond lengths from 2.193(2) to 2.263(2) Å in (**1**), Co–O bond lengths from 2.026(5) to 2.115(5) Å in (**2**) and much shorter Cu–O bond lengths from 1.942(2) to 1.999(3) Å in (**3**) and from 1.9213(19) to 1.9916(16) in (**4**). The coordination spheres around the Cd^{II} and Co^{II} ions in (**1**) and (**2**), respectively, are completed by one H_2O (Cd–O10 2.321(2) Å; Co–O10 2.092(5) Å) and one ^iPrOH (Cd–O9 2.309(2) Å; Co–O9 2.115(5) Å). In (**3**), the coordination sphere of each Cu^{II} ion is completed by two MeCN molecules with Cu-N bond lengths which range from 1.984(4) to 2.354(3) Å. The coordination sphere of Cu1 in (**4**) are completed by one H_2O (Cu1–O16 1.939(2) Å) and one 68:32 disordered ^iPrOH:DMF (Cu1–O17A/B 2.509(4)/2.336(14) Å). For Cu2 the coordination is provided by ordered solvent molecules *i.e.* by one ^iPrOH (Cu2–O19 2.2636(19) and one DMF (Cu2–O18 1.9691(18) Å).

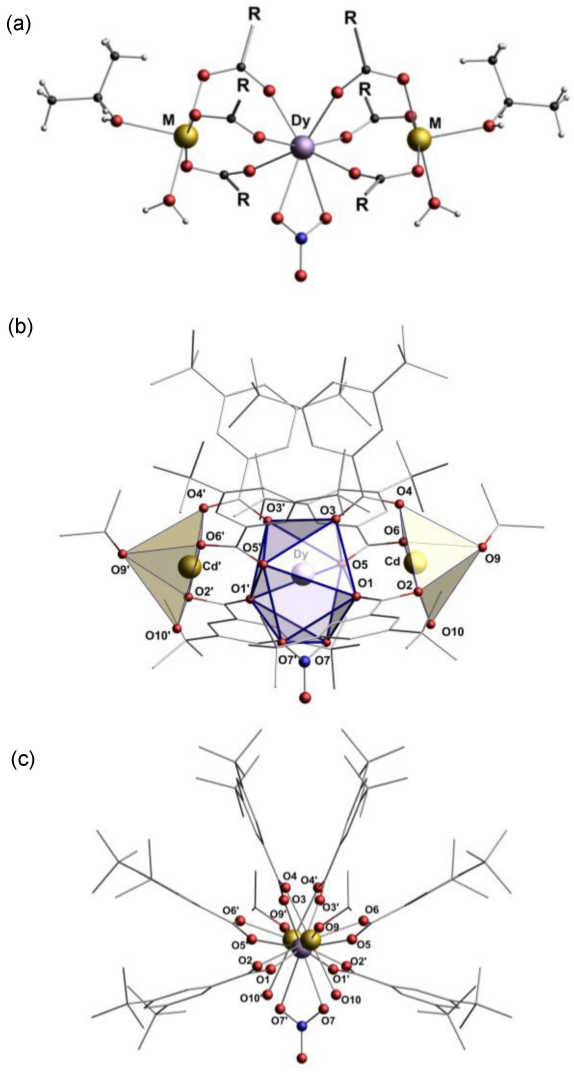

Figure 1. (a) Molecular structure of $[Cd_2Dy]$ (**1**) from the side view with R = 3,5-di-*tert*-butylphenyl. The core structures of (**1**) to (**4**) are identical regarding the bridging $dtbba^-$ ligands and the bidentate nitrate. The terminal ligands on the M^{II} ions (M=Cd for (**1**), Co for (**2**) and Cu for (**3**) and (**4**) are different from each other. (b) The molecular structure of (**1**) showing the coordination polyhedra. (c) The molecule from the front view. Hydrogen atoms and solvent molecules are omitted for clarity. Dy purple, Cd gold, O red, C black.

Table 1. Comparisons of terminal ligands, geometry around the metal ions, M–Dy–M angles and selected distances of (1) to (4).

Complex	(1) [Cd_2Dy]	(2) [Co_2Dy]	(3) [Cu_2Dy–MeCN]	(4) [Cu_2Dy–DMF]
M··M [Å]	7.5826(4)	7.5532(20)	7.4808(6)	7.5409(4)
Dy··M [Å]	3.8037(2)	3.8075(10)	3.7516(4), 3.7916(5)	3.8332(3), 3.8072(3)
M–Dy–M [°]	170.72(1)	165.40(3)	165.25(1)	161.48(1)
Terminal ligands on M	2×^{i}PrOH 2×H_2O	2×^{i}PrOH 2×H_2O	4×MeCN	1.7×^{i}PrOH 1×H_2O 1.3×DMF
Dy–O [Å]	2.277(2)–2.543(2)	2.246(5)–2.545(5)	2.258(2)–2.500(3)	2.2715(16)–2.5343(19)
M–O/M–N [Å]	2.193(2)–2.321(2)	2.026(5)–2.115(5)	1.942(2)–1.999(3)/1.984(4)–2.354(3)	1.9213(19)–2.509(4)
Geometry (Dy), deviation [%]	D_{2d} (TDD) 1.670	D_{2d} (TDD) 1.689	D_{2d} (TDD) 1.478	D_{2d} (TDD) 1.485
Geometry (M), deviation [%]	C_{4v} (VOC) 0.269	C_{4v} (VOC) 0.295	C_{4v} (SPY) 0.737 and 0.636	C_{4v} (SPY/VOC) $1.910^{017\,A}$/ 1.246^{017B} and 0.907

This leads to 5-coordinate M^{II} ions with a C_{4v} symmetry around the M^{II} ions and an O_5 environment in (**1**), (**2**) and (**4**) and to an O_3N_2 environment in (**3**). The coordination spheres can best be described as vacant octahedral (VOC) for the Cd^{II} ions in (**1**) and for the Co^{II} ions in (**2**). The coordination spheres around the Cu^{II} ions in (**3**) and (**4**) can be best described as either vacant octahedra (vOC) or spherical square pyramids (SPY) according to SHAPE 2.1 analysis (see Figure S7).[30] Comparisons of terminal ligands, geometry around the metal ions, M–Dy–M angles and selected bond distances for (**1**)–(**4**) are given in Table 1.

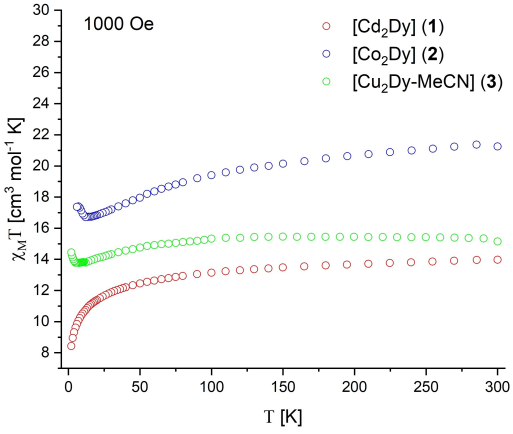

Figure 2. Susceptibility measurements of (**1**) (**2**) and (**3**) in a $\chi_M T$ versus T plot.

Magnetic properties

Susceptibility measurements were performed on polycrystalline samples immobilised in eicosane. The susceptibility data were corrected for the sample holder and the diamagnetic contribution including Pascal's constants.[31] For the investigation of the magnetic interactions of the systems, the $\chi_M T$ versus T plots for [Cd_2Dy] (**1**), [Co_2Dy] (**2**) and [Cu_2Dy–MeCN] (**3**) are shown in Figure 2. The experimental $\chi_M T$ product at 300 K is 13.97 $cm^3 K mol^{-1}$ for (**1**) which is in good agreement with the theoretical value of 14.17 $cm^3 K mol^{-1}$ for one Dy^{3+} with S = 5/2, g = 4/3, C = 14.17 $cm^3 K mol^{-1}$. The $\chi_M T$ product at 300 K for (**2**) is 21.25 $cm^3 K mol^{-1}$ which is higher than the value calculated (17.92 $cm^3 K mol^{-1}$) for two non-interacting spin-only high spin Co^{2+} with S = 3/2, g = 2.0, C = 1.875 $cm^3 K mol^{-1}$ and one Dy^{3+} with S = 5/2, g = 4/3, C = 14.17 $cm^3 K mol^{-1}$. This is doubtless the result of significant contributions from spin-orbit coupling of the Co^{II} ions which is not unexpected given the improbability of a g-value of 2.0 for Co^{II}.[32–37] For further theoretical background about the extraordinary magnetic behaviour of Co^{II} we refer the interested reader to other publications.[36,38–40] The $\chi_M T$ product 15.14 $cm^3 K mol^{-1}$ for (**3**) at 300 K is in good agreement with the theoretical value of 14.92 $cm^3 K mol^{-1}$ for two non-interacting Cu^{II} with S = 1/2, g = 2.0, C = 0.375. On decreasing the temperature, the $\chi_M T$ product for (**1**) is decreasing continuously to a value of 8.43 $cm^3 K mol^{-1}$ at 2 K and is likely due to depopulation of excited M_j states. The $\chi_M T$ product for (**2**) decreases to a value of 16.71 $cm^3 K mol^{-1}$ at 12 K, then increases to 17.37 $cm^3 K mol^{-1}$ at 6 K. The $\chi_M T$ product of (**3**) remains almost unchanged down to 100 K, decreases slightly with decreasing temperature to a value of 13.77 $cm^3 K mol^{-1}$ at 7 K and then increases to a value of 14.44 $cm^3 K mol^{-1}$ at 2 K. The increase of the $\chi_M T$ products for (**2**) and (**3**) at low temperatures suggest the coexistence of weak ferromagnetic interactions. By contrast, in a superficially similar "in-line" Co^{II}_2Dy complex, a down-turn in $\chi_M T$ at low temperature was ascribed to antiferromagnetic coupling.[24] However, in this compound the Co^{II} have tetrahedral geometries, as opposed to square-pyramidal in (**2**), which will have significant effects on the Co^{II} g-matrices,[40] and the Co–Dy–Co angle deviates much more strongly from linearity than for (**2**).

The anisotropy axis of the Dy^{III} ion for (**1**) was calculated using MAGELLAN[41] and is given in Figure 3. Additional ac susceptibility measurements for [Cd_2Dy] (**1**), [Co_2Dy] (**2**) and [Cu_2Dy–MeCN] (**3**) at 2 K do not show slow relaxation of magnetisation in the measurement window from 1 to 1500 Hz under zero field nor applied fields of 500, 1000, 1500 and

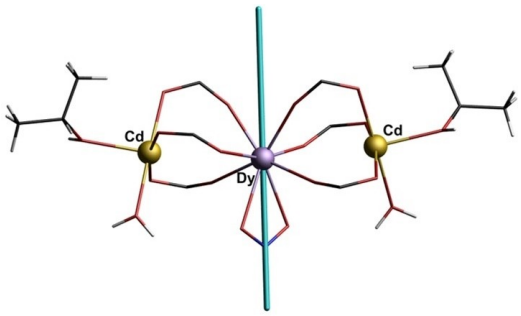

Figure 3. Anisotropy axis of the Dy^{III} ion for (**1**) calculated using MAGELLAN.

2000 Oe. The in-phase and out-of-phase susceptibilities for (**1**), (**2**) and (**3**) are shown in the supplementary information (Figure S 1, S 2 and S 3).

Conclusions

We have presented four new structures of the form $[M_2Dy]$ with M = Cd, Co and Cu with an almost linear arrangement with M–Dy–M angles of 170.7° in (**1**) $[Cd_2Dy]$, 165.4° in (**2**) $[Co_2Dy]$, 165.2° in (**3**) $[Cu_2Dy–MeCN]$ and 161.4° in (**4**) $[Cu_2Dy–DMF]$. It could be found that the M··M distance increases with increasing M–Dy–M angle in (**1**), (**2**) and (**3**), the only exception here is in (**4**). The dc susceptibility measurements for (**1**), (**2**) and (**3**) suggest that there are effects of ferromagnetic interactions in (**2**) and (**3**). Slow relaxation of magnetization could not be observed for the investigated complexes. The geometry around the Dy^{III} ions in the discussed systems is D_{2d} symmetry with an O_8 environment. The Cd^{II} and Co^{II} ions in (**1**) and (**2**) are 5-coordinate and their coordination spheres are close to vacant octahedra with very small deviations from the idealised geometry. The coordination spheres for the Cu^{II} ions in (**3**) and (**4**) are also 5-coordinate but better described as SPY, *i.e.* the Cu^{II} is not in the plane of the square-based pyramid.

Experimental Section

General information. All of the chemicals and solvents used for synthesis were obtained from commercial sources and used as received without further purification except of the dysprosium salts which were synthesized with the corresponding acid and Dy_2O_3. For the C/H/N Elemental Analysis the device Vario Micro Cube from Perkin Elmer was used. Fourier transform IR spectra in a range from 4000 to 400 cm^{-1} were measured on a Platinum Alpha ATR from Bruker with a resolution of 1 cm^{-1}. Magnetic measurements were performed on a MPMS-XL5 SQUID magnetometer from Quantum Design in the temperature ranges 6-300 K for (**2**) and 2-300 K for (**3**) under an external magnetic field of 1000 Oe. To check phase purity powder diffraction patterns were collected using a Stoe STADI-P diffractometer with a Cu–K_α source with λ = 1.5405 Å and were processed using the software $WinX^{POW}$. Simulated patterns were generated using Mercury 2020.1. The comparison of experimental and simulated powder patterns of (**1**)–(**4**) are shown in Figure S4 and Figure S5.

X-ray analysis. X-ray crystallographic data were collected using an Agilent SuperNova diffractometer with a Cu-K_a source λ = 1.54184 cm^{-1} on a CCD detector (EOS) or using a Stoe StadiVari diffractometer with a Mo-K_α source λ = 0.71073 cm^{-1} on a CMOS detector (Dectris Pilatus 300 K). The crystals were attached to the goniometer head with perfluoro ether oil. The data were integrated and corrected for Lorentz-polarisation and crystal absorption effects. The structure determination and refinement were performed using SHELXL-2018[42] and the program OLEX2.[43] Crystallographic data of (**1**)–(**4**) are given in Table 2.

Full crystallographic data and details of the structural determinations for the structures in this paper have been deposited with the Cambridge Crystallographic Data Centre as supplementary publication nos. CCDC 2157725-2157728. Copies of the data can be obtained, free of charge, from https://www.ccdc.cam.ac.uk/structures/.

*Synthesis of $[Cd_2Dy(dtbba)_6(^iPrOH)_2(H_2O)_2NO_3]\cdot {}^iPrOH$ (**1**):* 173 mg 3,5-di-*tert*-butylbenzoic acid (0.74 mmol) and 110 µL triethylamine (0.80 mmol) were added to a solution of 110 mg $Dy(NO_3)_3\cdot 6H_2O$ (0.24 mmol) and 61 mg $Cd(NO_3)_2\cdot 4H_2O$ (0.20 mmol) in MeCN:^{i}PrOH (10:10 mL). The colourless solution was heated for 1.5 h at 80 °C, then filtered. White X-ray suitable crystals were obtained after 20 days of slow solvent evaporation. Yield: 132 mg (26% based on Dy). Elemental analysis for $Cd_2DyC_{102}H_{162}NO_{21}$: Calc% (found%) C/H/N: 57.63(57.24), 7.68(7.33), 0.66(0.62). Selected IR peaks (cm^{-1}): $\tilde{\nu}$ = 2964 (s), 2902 (m), 2865 (m), 1562 (s), 1397 (vs), 1290 (s), 788 (s), 741 (s), 703 (s).

*Synthesis of $[Co_2Dy(dtbba)_6(^iPrOH)_2(H_2O)_2NO_3]\cdot {}^iPrOH$ (**2**):* 173 mg 3,5-di-*tert*-butylbenzoic acid (0.74 mmol) and 110 µL triethylamine (0.79 mmol) were added to a solution of 110 mg $Dy(NO_3)_3\cdot 6H_2O$ (0.24 mmol) and 50 mg $Co(NO_3)_2\cdot 6H_2O$ (0.17 mmol) in MeCN:^{i}PrOH (30:10 mL). The blue solution was heated for 30 minutes at 80 °C, then filtered. Purple X-ray suitable crystals were obtained after 20 days of slow solvent evaporation. Yield: 85 mg (18% based on Dy). Elemental analysis for $Co_2DyC_{102}H_{162}NO_{21}$: Calc%(found%) C/H/N: 60.69(59.99), 8.09(7.79), 0.69(0.61). Selected IR peaks (cm^{-1}): $\tilde{\nu}$ = 2964 (s), 2902 (m), 2865 (m), 1570 (s), 1437 (s), 1397 (vs), 128 (s), 790 (s), 734 (s), 703 (s).

*Synthesis of $[Cu_2Dy(dtbba)_6(MeCN)_4NO_3]\cdot MeCN$ (**3**):* 117 mg 3,5-di-*tert*-butylbenzoic acid (0.50 mmol) and 69 µL triethylamine (0.50 mmol) were added to a solution of 38 mg $Dy(NO_3)_3\cdot 6H_2O$ (0.08 mmol) and 40 mg $Cu(NO_3)_2\cdot 2{,}5H_2O$ (0.17 mmol) in MeCN:^{i}PrOH (30:10 mL). The blue solution was heated for 1.5 hours at 80 °C, then filtered. Blue X-ray suitable crystals were obtained after 20 days of slow solvent evaporation. Yield: 54 mg (34% based on Dy). Elemental analysis for $Cu_2DyC_{102}H_{144}N_7O_{15}$: Calc%(found%) C/H/N: 61.32(60.95), 7.26(7.45), 4.91(4.82). Selected IR peaks (cm^{-1}): $\tilde{\nu}$ = 2964 (s), 2902 (m), 2865 (m), 1574 (vs), 1442 (vs), 1391 (vs), 1288 (s), 896 (s), 790 (s), 738 (s), 704 (s).

*Synthesis of $[Cu_2Dy(dtbba)_6(^iPrOH)_2(H_2O)(DMF)NO_3]\cdot 3\ {}^iPrOH\cdot H_2O$ (**4**):* 146 mg 3,5-di-*tert*-butylbenzoic acid (0.62 mmol) and 91.6 µL triethylamine (0.66 mmol) were added to a solution of 91 mg $Dy(NO_3)_3\cdot 6H_2O$ (0.20 mmol) and 36 mg $Cu(NO_3)_2\cdot 2.5H_2O$ (0.15 mmol) in ^{i}PrOH:DMF (30:1 mL). The blue solution was heated for 30 minutes at 80 °C, then filtered. Blue X-ray suitable crystals were obtained after 40 days of slow solvent evaporation. Yield: 149 mg (34% based on Dy). Elemental analysis for $Cu_2DyC_{108}H_{176}N_2O_{23}$: Calc%(found%) C/H/N: 60.05(59.95), 8.21(8.08), 1.30(1.27). Selected IR peaks (cm^{-1}): $\tilde{\nu}$ = 2964 (s), 2902 (m), 2865 (m), 1654 (s), 1570 (vs), 1438 (s), 1397 (vs), 1288 (s), 893 (m), 790 (s), 736 (s), 704 (s).

Table 2. Crystallographic data of (**1**)–(**4**).

Complex	(**1**)	(**2**)	(**3**)	(**4**)
Formula	Cd_2Dy $C_{102}H_{162}NO_{21}$	Co_2Dy $C_{102}H_{162}NO_{21}$	Cu_2Dy $C_{102}H_{144}N_7O_{15}$	Cu_2Dy $C_{108}H_{176.75}N_{2.25}O_{23}$
M [g/mol]	2125.62	2018.68	1997.81	2164.40
T [K]	293(2)	180(2)	180(2)	180(2)
Crystal system	monoclinic	monoclinic	triclinic	triclinic
Space group	C2/c	C2/c	P-1	P-1
a [Å]	18.5458(3)	18.2495(18)	14.2576(3)	15.9987(4)
b[Å]	28.9861(5)	28.5069(16)	17.3464(5)	16.8223(5)
c[Å]	21.3566(3)	21.385(2)	25.1026(7)	23.9767(6)
α[°]	90	90	83.292(2)	94.298(2)
β[°]	94.455(2)	93.882(8)	81.049(2)	94.192(2)
γ[°]	90	90	73.948(2)	114.319(2)
V/[Å]^3	11446.0(3)	11099.8(17)	5875.8(3)	5825.3(3)
Z	4	4	2	2
ρ_{calc} [g/cm^3]	1.234	1.208	1.129	1.234
μ [mm^{-1}]	6.868	1.023	1.043	1.061
F(000)	4444	4276	2098	2297
Radiation	CuKα (λ = 1.54184)	MoKα (λ = 0.71073)	MoKα (λ = 0.71073)	MoKα (λ = 0.71073)
Refl. collected/ unique	25355/ 10827	29613/ 11668	78155/ 34689	59290 /32941
R(int)/ R(sigma)	0.0190/ 0.0248	0.0978/ 0.1036	0.0294/ 0.0473	0.0315/ 0.0641
Data/restraints/ parameters	10827/3/ 606	11668/5/ 606	34689/13/ 1140	32941/77/ 1315
GOF on F^2	1.041	1.021	1.036	0.968
R_1/wR_2 [I > 2σ (I)]	0.0317/ 0.0804	0.0960/ 0.2404	0.0569/ 0.1613	0.0402/ 0.0903
R_1/wR_2 (all data)	0.0416/ 0.0873	0.1374/ 0.2771	0.0813/ 0.1789	0.0685/ 0.0983
Largest difference peak/hole [eÅ^{-3}]	0.78/−0.87	3.93/−3.33	1.39/−1.42	1.41/−0.76

Acknowledgements

We thank the DFG SFB/TRR 88 3MET, the Helmholtz Foundation for funding through POF STN. The authors thank Prof. Dr. Dieter Fenske for all his support over the years. Open Access funding enabled and organized by Projekt DEAL.

Conflict of Interest

The authors declare no conflict of interest.

Data Availability Statement

The data that support the findings of this study are available in the supplementary material of this article.

Keywords: Heterometallic complexes transition metals · lanthanides · magnetic properties

[1] J. D. Rinehart, J. R. Long, *Chem. Sci.* **2011**, *2*, 2078–2085.
[2] T. Kajiwara, M. Nakano, K. Takahashi, S. Takaishi, M. Yamashita, *Chem. Eur. J.* **2011**, *17*, 196–205.
[3] M. Maeda, S. Hino, K. Yamashita, Y. Kataoka, M. Nakano, T. Yamamura, T. Kajiwara, *Dalton Trans.* **2012**, *41*, 13640–13648.
[4] Y. S. Meng, S. D. Jiang, B. W. Wang, S. Gao, *Acc. Chem. Res.* **2016**, *49*, 2381–2389.
[5] A. Dey, J. Acharya, V. Chandrasekhar, *Chem. Asian J.* **2019**, *14*, 4433–4453.
[6] V. Chandrasekhar, B. M. Pandian, R. Azhakar, J. J. Vittal, R. Clerac, *Inorg. Chem.* **2007**, *46*, 5140–5142.
[7] S. Osa, T. Kido, N. Matsumoto, N. Re, A. Pochaba, J. Mrozinski, *J. Am. Chem. Soc.* **2004**, *126*, 420–421.
[8] V. M. Mereacre, A. M. Ako, R. Clerac, W. Wernsdorfer, G. Filoti, J. Bartolome, C. E. Anson, A. K. Powell, *J. Am. Chem. Soc.* **2007**, *129*, 9248–9249 + +
[9] V. Mereacre, M. N. Akhtar, Y. H. Lan, A. M. Ako, R. Clerac, C. E. Anson, A. K. Powell, *Dalton Trans.* **2010**, *39*, 4918–4927.
[10] C. J. Li, Z. J. Lin, M. X. Peng, J. D. Leng, M. M. Yang, M. L. Tong, *Chem. Commun.* **2008**, *44*, 6348–6350.
[11] Y. Liu, Y. C. Chen, J. Liu, W. B. Chen, G. Z. Huang, S. G. Wu, J. Wang, J. L. Liu, M. L. Tong, *Inorg. Chem.* **2020**, *59*, 687–694.
[12] Y. Peng, V. Mereacre, C. E. Anson, A. K. Powell, *Dalton Trans.* **2017**, *46*, 5337–5343.
[13] E. M. Pineda, N. F. Chilton, F. Tuna, R. E. P. Winpenny, E. J. L. McInnes, *Inorg. Chem.* **2015**, *54*, 5930–5941.
[14] M. A. Shmelev, N. V. Gogoleva, D. A. Makarov, M. A. Kiskin, I. A. Yakushev, F. M. Dolgushin, G. G. Aleksandrov, E. A. Varaksina,

I. V. Taidakov, E. V. Aleksandrov, A. A. Sidorov, I. L. Eremenko, *Russ. J. Coord. Chem.* **2020**, *46*, 1–14.
[15] J. Goura, J. Brambleby, P. Goddard, V. Chandrasekhar, *Chem. Eur. J.* **2015**, *21*, 4926–4930.
[16] A. Upadhyay, S. K. Singh, C. Das, R. Mondol, S. K. Langley, K. S. Murray, G. Rajaraman, M. Shanmugam, *Chem. Commun.* **2014**, *50*, 8838–8841.
[17] M. A. Palacios, S. Titos-Padilla, J. Ruiz, J. M. Herrera, S. J. A. Pope, E. K. Brechin, E. Colacio, *Inorg. Chem.* **2014**, *53*, 1465–1474.
[18] D. F. Lu, X. J. Kong, T. B. Lu, L. S. Long, L. S. Zheng, *Inorg. Chem.* **2017**, *56*, 1057–1060.
[19] G. L. Zhang, S. Wang, J. L. Hou, C. J. Mo, C. J. Que, Q. Y. Zhu, J. Dai, *Dalton Trans.* **2016**, *45*, 17681–17686.
[20] S. T. Wu, B. B. Deng, X. L. Jiang, R. H. Li, J. B. Guo, F. L. Lai, X. H. Huang, C. C. Huang, *J. Solid State Chem.* **2012**, *196*, 451–457.
[21] Y. Zhu, F. Luo, Y. M. Song, X. F. Feng, M. B. Luo, Z. W. Liao, G. M. Sun, X. Z. Tian, Z. J. Yuan, *Cryst. Growth Des.* **2012**, *12*, 2158–2161.
[22] H. H. Nguyen, J. J. Jegathesh, A. Takiden, D. Hauenstein, C. T. Pham, C. D. Le, U. Abram, *Dalton Trans.* **2016**, *45*, 10771–10779.
[23] X. J. Zhang, K. Liu, Y. M. Bing, N. Xu, W. Shi, P. Cheng, *Dalton Trans.* **2015**, *44*, 7757–7760.
[24] M. Kiskin, E. Zorina-Tikhonova, S. Kolotilov, A. Goloveshkin, G. Romanenko, N. Efimov, I. Eremenko, *Eur. J. Inorg. Chem.* **2018**,1356–1366.
[25] C. M. Liu, D. Q. Zhang, X. Hao, D. B. Zhu, *Chem. Asian J.* **2014**, *9*, 1847–1853.
[26] T. Yamaguchi, J. P. Costes, Y. Kishima, M. Kojima, Y. Sunatsuki, N. Brefuel, J. P. Tuchagues, L. Vendier, W. Wernsdorfer, *Inorg. Chem.* **2010**, *49*, 9125–9135.
[27] G. Novitchi, S. Shova, A. Caneschi, J. P. Costes, M. Gdaniec, N. Stanica, *Dalton Trans.* **2004**, 1194–1200.
[28] P. Mahapatra, S. Ghosh, N. Koizumi, T. Kanetomo, T. Ishida, M. G. B. Drew, A. Ghosh, *Dalton Trans.* **2017**, *46*, 12095–12105.
[29] Y. Zhu, F. Luo, X. F. Feng, Z. W. Liao, Y. M. Song, H. X. Huang, X. Z. Tian, G. M. Sun, M. B. Luo, *Aust. J. Chem.* **2013**, *66*, 75–83.
[30] S. Alvarez, P. Alemany, D. Casanova, J. Cirera, M. Llunell, D. Avnir, *Coord. Chem. Rev.* **2005**, *249*, 1693–1708.
[31] G. A. Bain, J. F. Berry, *J. Chem. Educ.* **2008**, *85*, 532–536.
[32] G. K. Gransbury, M. E. Boulon, R. A. Mole, R. W. Gable, B. Moubaraki, K. S. Murray, L. Sorace, A. Soncini, C. Boskovic, *Chem. Sci.* **2019**, *10*, 8855–8871.
[33] A. M. Bryan, W. A. Merrill, W. M. Reiff, J. C. Fettinger, P. P. Power, *Inorg. Chem.* **2012**, *51*, 3366–3373.
[34] K. Fink, C. Wang, V. Staemmler, *Inorg. Chem.* **1999**, *38*, 3847–3856.
[35] M. Murrie, *Chem. Soc. Rev.* **2010**, *39*, 1986–1995.
[36] M. Murrie, S. J. Teat, H. Stoeckli-Evans, H. U. Gudel, *Angew. Chem. Int. Ed.* **2003**, *42*, 4653–4656; *Angew. Chem.* **2003**, *115*, 4801–4804.
[37] K. C. Mondal, A. Sundt, Y. H. Lan, G. E. Kostakis, O. Waldmann, L. Ungur, L. F. Chibotaru, C. E. Anson, A. K. Powell, *Angew. Chem. Int. Ed.* **2012**, *51*, 7550–7554; *Angew. Chem.* **2012**, *124*, 7668–7672.
[38] F. Lloret, M. Julve, J. Cano, R. Ruiz-Garcia, E. Pardo, *Inorg. Chim. Acta* **2008**, *361*, 3432–3445.
[39] Y. Peng, V. Mereacre, C. E. Anson, Y. Q. Zhang, T. Bodenstein, K. Fink, A. K. Powell, *Inorg. Chem.* **2017**, *56*, 6056–6066.
[40] F. Klower, Y. H. Lan, J. Nehrkorn, O. Waldmann, C. E. Anson, A. K. Powell, *Chem. Eur. J.* **2009**, *15*, 7413–7422.
[41] N. F. Chilton, D. Collison, E. J. L. McInnes, R. E. P. Winpenny, A. Soncini, *Nat. Commun.* **2013**, *4*.
[42] G. M. Sheldrick, *Acta Crystallogr. Sect. C* **2015**, *71*, 3–8.
[43] O. V. Dolomanov, L. J. Bourhis, R. J. Gildea, J. A. K. Howard, H. Puschmann, *J. Appl. Crystallogr.* **2009**, *42*, 339–341.

Manuscript received: March 11, 2022
Revised manuscript received: May 23, 2022
Accepted manuscript online: May 30, 2022

